Daduí C. Guerrieri[1]
Space Engineering Department,
Faculty of Aerospace Engineering,
Delft University of Technology,
Delft 2629 HS, The Netherlands
e-mail: D.CordeiroGuerrieri@tudelft.nl

Marsil A. C. Silva
Space Engineering Department,
Faculty of Aerospace Engineering,
Delft University of Technology,
Delft 2629 HS, The Netherlands

Angelo Cervone
Space Engineering Department,
Faculty of Aerospace Engineering,
Delft University of Technology,
Delft 2629 HS, The Netherlands

Eberhard Gill
Space Engineering Department,
Faculty of Aerospace Engineering,
Delft University of Technology,
Delft 2629 HS, The Netherlands

Selection and Characterization of Green Propellants for Micro-Resistojets

The number of launches of nano- and pico-satellites has significantly increased over the past decade. Miniaturized subsystems, such as micropropulsion, for these classes of spacecraft are rapidly evolving and, in particular, micro-resistojets have shown great potential of applicability. One of the key points to address in the development of such devices is the propellants selection, since it directly influences the performance. This paper presents a methodology for the selection and characterization of fluids that are suitable for use as propellants in two micro-resistojet concepts: vaporizing liquid micro-resistojet (VLM) and the low-pressure micro-resistojet (LPM). In these concepts, the propellant is heated by a nonchemical energy source, in this case an electrical resistance. In total 95 fluids have been investigated including conventional and unconventional propellants. A feasibility assessment step is carried out following a trade-off using a combination of the analytical hierarchy process (AHP) and the Pugh matrix. A final list of nine best-scoring candidates has been analyzed in depth with respect to the thermal characteristics involved in the process, performance parameters, and safety issues. For both concepts, water has been recognized as a very promising candidate along with other substances such as ammonia and methanol. [DOI: 10.1115/1.4036619]

1 Introduction

The market of very small satellites in the classes of nano- and pico-satellites (less than 10 kg) is rapidly growing. Although used in the beginning primarily as an educational tool, they have recently become attractive also for various scientific or commercial applications. The standardization of this class of satellites is based on well-known form factors such as the CubeSat and, more recently, the PocketQube. It allows for using commercial-off-the-shelf (COTS) technologies, decreasing the development time and cost [1–3]. Even though the number of available COTS components for these satellites is rapidly increasing, there is still a lack of sufficient choices of micropropulsion systems for them.

Many micropropulsion devices have been developed in recent years in an attempt to provide CubeSats with the mentioned capabilities. Among these systems, we can highlight some of the most promising ones due to aspects such as reliability and simplicity: pulsed-plasma thrusters (PPT) [4,5], cold-gas thrusters [6], and micro-resistojets [7–9]. This paper will focus in particular on micro-resistojets, propulsion devices, where a given fluid is heated to a higher temperature (and eventually vaporized, if necessary) by an electric resistance, before being accelerated in a nozzle.

Some recent studies have proven that the micro-resistojet is a promising propulsion system for those classes of satellites, allowing them to perform missions that include formation flying, station keeping of constellations, and orbit transfer [10]. The main reasons are their high integration capability, small volume, low mass, fast response, high thrust to mass ratio, high reliability, and easy integrability in a thruster array. In addition, they can easily achieve a thrust level in the range of 1–10 mN with a specific impulse in the range of 50–200 s, and a reasonably low power consumption [9].

The Space System Engineering chair at Delft University of Technology (TU Delft) is currently developing two kinds of micro-resistojet, abbreviated in this paper as VLM and LPM. The main difference between them is the level of pressure at which they work: while the VLM works in a range from 200 kPa to 500 kPa in the chamber, the LPM works in the range from 50 Pa to 300 Pa. This means that they have a different operational principle: continuous flow regime for the VLM (Knudsen number lower than 0.1) and transitional regime for the LPM (Knudsen number between 0.1 and 10). Both concepts can meet the requirements for orbit maintenance, transfer, formation flying, and/or attitude control of nano- and pico-satellites. Additionally, it is possible to meet safety requirements in terms of pressure, corrosivity, flammability, and toxicity, with a well-selected propellant [9].

A trend toward "green" space systems has attracted the attention of the space community. All the roadmaps of space agencies urge the need of moving toward that [11,12]. Many propellants are known for the high-potential hazards in a propulsion system. One well-known example is hydrazine, which is both toxic and carcinogenic. According to Ref. [13], space agencies have tried to find an alternative to these propellants, as an important step toward a low hazard and reduced cost and a way to provide viable and safer alternatives to the space industry.

Recently, the PRISMA mission implementing two microsatellites flying in formation made the first flight demonstration of a new "high-performance green propellant" as a potential substitute of the traditional hydrazine [14]. Other green in-orbit demonstration propulsion systems were, in cold gas thrusters, Xenon and Nitrogen (on board, as examples, of the Orbcomm, Inspector, Rapideye, and UK-DMC satellites), and in resistojet propulsion systems butane and nitrous oxide (on board of UK-DMC, UoSAT-12, and Alsat-1 [15]). In the class of very small satellites, the most commonly used thrusters so far are cold gas systems, and flight demonstrations have been carried out for instance by CanX-2 [16] and Delfi-N3xt [3].

More in general, in Ref. [17], the authors present nitrous oxide. They compare it to other typical propellants such as ammonia, carbon dioxide, and water. They show nitrous oxide as a

[1]Corresponding author.

Contributed by the Heat Transfer Division of ASME for publication in the Journal of Heat Transfer. Manuscript received December 6, 2016; final manuscript received April 19, 2017; published online May 23, 2017. Editor: Portonovo S. Ayyaswamy.

promising green propellant which provides a high performance and is nontoxic, nonflammable, and noncorrosive. Even though nitrous oxide is classified as a liquefied gas, the order of pressure to keep it as a liquid is 5.24 MPa (52.4 bar) at 21 °C, which is a challenge to use on nano- and pico-satellites.

Due to the significant high number of potential choices, propellant selection is a difficult trade-off between performance, safety, and any other desired features, such as density, heat capacity, storability, and availability [18]. A selection methodology is proposed in this paper to provide a fair comparison of propellants in the specific case of micro-resistojets. This methodology is divided into four steps: (1) data collection of the 95 fluids that have been selected, (2) feasibility assessment to discard unfeasible fluids in terms of storage, (3) AHP tool [19] with Pugh matrix [20] comparison to classify the selected feasible fluids in terms of safety and design, and (4) final analysis regarding thermal characteristics, propulsive performance, and safety.

2 Requirements

The miniaturization of satellites creates constraints mainly in size, mass, and power that have to be taken into account when designing propulsion subsystems. Moreover, those satellites are usually put into orbit by piggy-back launches and, due to that, launch providers impose a number of constraints related to the safety of the main payload of the rocket. Other constraints come from the standardization of these satellite classes as well as the specific mission.

We can consider as an example the requirements proposed in Ref. [21] for a formation flying mission, see Table 1. Each mission has its own specific requirements, but the ones listed in the table represent a good example of a typical formation flying mission in low-altitude orbits, which is expected to become a more and more common type of mission for small satellites. These requirements will be used as a reference along the paper.

From these suggested requirements, we can derive guidelines for the propellant selection. The main points of interest regard performance (associated mainly to thrust and specific impulse), system density (associated to mass and size), and safety. Other characteristics such as power consumption can be more relaxed as they also depend on other factors, such as structural design, solar panel design, mission design, and operation management (for example, the operation of the engines can be restricted to when the batteries are full or during eclipse).

The safety level can be divided, in turn, into flammability, instability, and health hazard, and it is discussed here based on the possible consequences of these different aspects. The flammability and instability of the propellant have two main consequences: one is the reduction of the satellites' reliability and the other associated to the risks for the main payload (in case of a piggy-back launch). The health hazard concerns the propellant handling before launch. This can be seen from two different perspectives, depending on whether the satellite is assembled by integrator companies, that normally have the proper facilities to handle hazardous propellants, or by Academic groups, that usually have more limitation on this kind of facilities and prioritize the safety of their students and researchers.

Table 1 DelFFi propulsion system requirements [21]

Parameter	Value
Thrust (mN)	0.5–9.5
Delta-V (m/s)	>15
Total mass (g)	<459
Peak power consumption (W)	6.0
Total energy consumption per day (kJ)	<100
Internal pressure (bar)	<10
Total size (mm)	$< 90 \times 90 \times 80$
Pyrotechnic devices	No
Hazardous propellants	No

3 Selection Methodology

The methodology to select the most suitable propellant is based on four sequential steps:

(1) data collection
(2) feasibility assessment
(3) AHP and Pugh matrix
(4) analysis

The first step is to collect data on all realistic fluids that could be used as propellants in micro-resistojet systems. The second step is to select, among the identified fluids, only the ones which might be feasible to work on. The third step is to use the AHP combined with a Pugh matrix tool to compare the remaining fluids with respect to the three main criteria: safety, performance, and system density. Finally, the fourth step is to analyze in a more detailed manner the substances that score the highest in the previous step.

In the data collection step, a total of 95 fluids used in engineering applications were considered, including single and compound chemical substances. These include not only the fluids typically used as refrigerants, fuels, propellants, oxidizers but also the fluids used in everyday life. The list of all fluids can be seen in the Appendix.

In the feasibility assessment step, the main criteria considered were as follows: the required pressure to correctly store the propellant in the tank and the required propellant mass. Looking at the requirements listed in Table 1, the only option is to store the propellant as a liquid or a solid, due to the low density achieved if stored as a gas at the required maximum pressure. The fluids which cannot be liquid or solid at a temperature of 293.15 K and pressure of 10 bar (1 MPa) or lower were discarded. In this stage, the most common fluids used by cold gas thrusters, such as nitrogen and carbon dioxide, were excluded.

The criteria selected for the Pugh matrix are classified into a first (FL) and second (SL) level. The first level includes the safety branch and design branch. The second level better specifies the safety criterion into flammability, instability, and health hazard, and the design one into performance and system density. The weighting factor (WF) for each criterion was defined by using the AHP tool. Figure 1 shows the decision hierarchy from how the weight ratio (WR) was considered. Five academic staff members from the Space System Engineering chair at TU Delft performed a pairwise comparison of the criteria in order to define the values of WF.

The WF considered in this work is ranged from 1 to 6, where 1 means least important and 6 means most important. For each criterion, based on the pairwise comparison, a different WF was defined in accordance to the resulted WR. It was done as follows:

$$\mathrm{WF}_i = \frac{\mathrm{WR}_i^{\mathrm{FL}}}{\mathrm{WR}_{\mathrm{max}^{\mathrm{FL}}}} \cdot \frac{\mathrm{WR}_i^{\mathrm{SL}}}{\mathrm{WR}_{\mathrm{max}^{\mathrm{SL}}}} \cdot \mathrm{WF}_{\mathrm{max}} \tag{1}$$

where i is the criteria, FL is the first level, SL is the second level, and the $\mathrm{WF}_{\mathrm{max}}$ is equal to 6 in this case. Table 2 presents the WF for each one of the evaluators that performed the pairwise comparison. Each of these WFs is used in different Pugh matrices resulting in different outcomes that are dependent on the specific values given by each evaluator.

The other element of the Pugh matrix is the scores given in each criterion to each fluid. The fluids were scored by + (positive), − (negative), or 0 (neutral) in all criteria.

From the safety perspective, Ref. [22] was used to derive the scores. All criteria indicated in this document were considered in the analysis except, for the sake of simplicity, the special hazards. If special hazards are present for a selected fluid, a specific

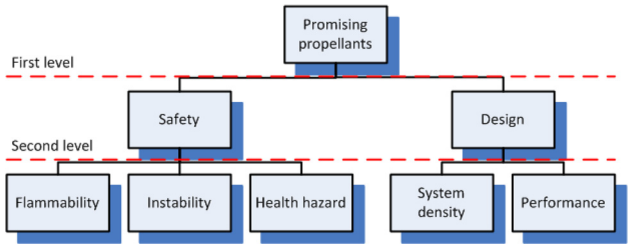

Fig. 1 The AHP resulting in the weight ratio for each criterion

additional analysis is expected to be done. The 0–4 range used in Ref. [22] to quantify the degree of hazard in each category was translated into a trade-off score by considering 2 as neutral (0), 0 and 1 as positive (+), and 3 and 4 as negative (–).

From the engineering perspective, a simplified first-order approximation was used. From the ideal rocket theory, it is known that the specific impulse is inversely proportional to the square root of the molecular mass. Using this approximation, a value lower than 30.5 g/mol is considered as positive (+), higher than 69.5 g/mol as negative (–), and between them as neutral (0). Looking at the system density, since the remaining fluids were in a range of density from 500.56 kg/m^3 to 1636.80 kg/m^3 at 283.15 K and 1 MPa, a density lower than 879.31 kg/m^3 was scored as positive (+), higher than 1258.05 kg/m^3 as negative (–), and between them as neutral (0). Those values were considered into the range between the lowest and the highest molecular mass or density divided by three.

With all settings defined, the Pugh matrix was completed for each evaluator with their different defined WF. Following this step, the Pugh matrix result for each fluid, specific of each evaluator, was used to make an average score and a standard deviation. After that, the result was used to select a final group of the most promising fluids.

This detailed analysis (final step of the selection method) has been carried out for the two different resistojet concepts, the VLM and the LPM. The performance factors considered in this analysis were the thrust, the specific impulse, and the power needed to heat up the propellant. The ideal rocket theory is used as a baseline to calculate the thrust $\Im$ and the specific impulse I_{sp}, by means of

$$\Im = \dot{m}v_e + (p_e - p_a)A_e \tag{2}$$

$$I_{sp} = \frac{\Im}{\dot{m}g_0} \tag{3}$$

where $\dot{m}$ is the mass flow rate, v_e is the exit velocity, p_e the exit pressure, p_a the outer ambient pressure, A_e the exit area, and g_0 the Earth's gravitational acceleration at sea level. Moreover, for each of the two micro-resistojet concepts considered, different methods are applied to define the mass flow rate, the exit velocity, and the exit pressure, due to the different fluid dynamics involved (the VLM works in the continuum flow regime and the LPM works in the transitional regime).

Table 2 Weight factor (WF) result of each evaluator from the pairwise comparison, compared to the average $\overline{WF}$ and standard deviation σ among all evaluators

WF	1	2	3	4	5	$\overline{WF}$	σ
Flammability	1.9	5.6	0.9	1.3	1.5	2.2	1.7
Health hazard	3.3	2.4	4.0	6.0	2.0	3.5	1.4
Instability	6.0	6.0	1.5	3.6	3.2	4.1	1.7
Performance	6.0	6.0	6.0	4.0	6.0	5.6	0.8
System density	4.0	4.0	4.0	2.7	6.0	4.1	1.1

3.1 Vaporizing Liquid Micro-Resistojet (VLM). The VLM follows the classical equations from the continuous flow regime, the energy conservation and ideal gas relationships according to Ref. [18]. The mass flow rate can be calculated as

$$\dot{m} = \frac{p_c \cdot A^*}{\sqrt{\frac{R_A}{M_w} \cdot T_c}} \cdot \Gamma \tag{4}$$

where p_c is the chamber pressure, A^* is the nozzle throat area, R_A is the universal gas constant, M_w is the molecular mass, T_c is the chamber temperature, and Γ is the Vandenkerckhove function of the specific heat ratio γ, defined as

$$\Gamma = \sqrt{\gamma \cdot \left(\frac{1+\gamma}{2}\right)^{\frac{1+\gamma}{1-\gamma}}} \tag{5}$$

In addition, the nozzle expansion ratio (ratio of the exit area to the throat area) is a function of the pressure ratio (ratio of exit pressure to chamber pressure), according to the following equation:

$$\frac{A_e}{A^*} = \frac{\Gamma}{\sqrt{\frac{2\gamma}{\gamma-1} \cdot \left(\frac{p_e}{p_c}\right)^{\frac{2}{\gamma}} \cdot \left[1 - \left(\frac{p_e}{p_c}\right)^{\frac{\gamma-1}{\gamma}}\right]}} \tag{6}$$

Finally, the nozzle exit velocity (jet velocity) can be calculated as

$$v_e = \sqrt{\frac{2\gamma}{\gamma-1} \cdot \frac{R_A}{M_W} \cdot T_c \cdot \left[1 - \left(\frac{p_e}{p_c}\right)^{\frac{\gamma-1}{\gamma}}\right]} \tag{7}$$

3.2 Low-Pressure Micro-Resistojet (LPM). The LPM follows the equations from the transitional flow regime, the energy conservation and ideal gas relationships according to Ref. [23]. The mass flow rate can be calculated, in this case, with

$$\dot{m} = \alpha p_0 \sqrt{\frac{M_W}{2\pi R_A T_0}} A_e \tag{8}$$

where α is the transmission coefficient (ratio of exit to inlet mass flow rate in the flow direction), p_0 is the initial plenum pressure, and T_0 is the initial plenum temperature. The free molecular flow theory is used to derive an equation for the exit velocity, as

$$v_e = \sqrt{\frac{\pi R_A T_w}{2M_W}} \tag{9}$$

where T_w is the temperature of the microchannel walls. Additionally, the exit pressure for this concept was estimated from the results obtained in Ref. [24], where it was shown that the pressure thrust (second term on the right-hand side of Eq. (2)) represents about 42% of the total thrust for a heater chip based on microchannels.

4 Application of the Methodology and Results

From the feasibility assessment step, 63 fluids were selected (see the complete table provided in the Appendix for more details). All those fluids were evaluated by means of a Pugh matrix, with different criteria and different weights based on the

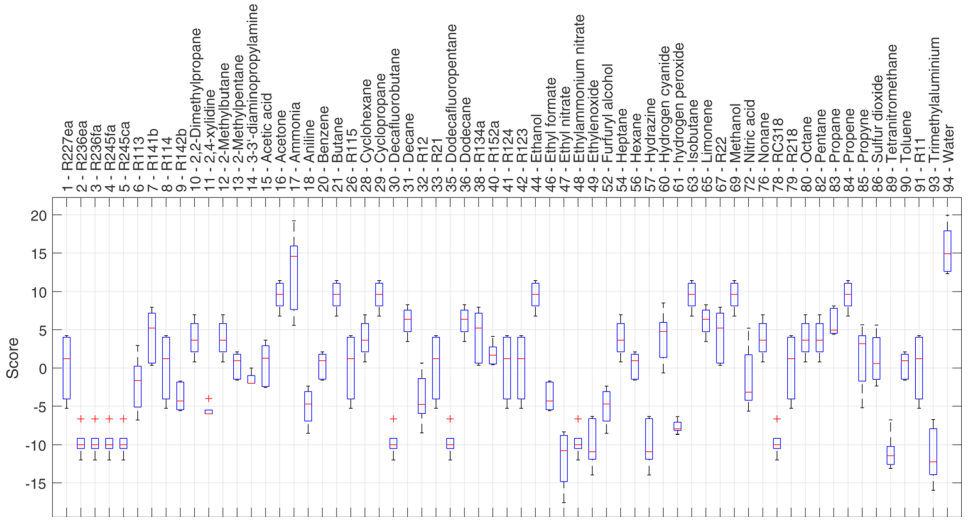

Fig. 2 Results of the Pugh matrix presented as a boxplot, where the middle line of the box represents the median, the upper and lower borders of the box represent the upper and lower quartiles, respectively, the top and bottom lines are the maximum and minimum value, and the crosses represent the outliers

evaluators perspectives, as explained in Sec. 3. The result of the Pugh matrix evaluation is shown by the boxplot in Fig. 2 in terms of average score and standard deviation of evaluations based on each expert's weights. The scores can go up to 30 which is the score for an ideal substance where all criteria score the maximum possible points (6). Similarly, a score of −30 represents the worst possible substance.

Based on the Pugh matrix results, the nine best-scored fluids were selected for further performance analysis, namely: acetone, ammonia, butane, cyclopropane, ethanol, isobutane, methanol, propene, and water. All other fluids, even in their best-case score, would receive less points than the worst-case score of any of these nine selected fluids.

Figure 3 shows the saturation curve of each selected fluid as a function of pressure and temperature. Even though the saturation curve allows us to understand the thermodynamic state of the fluid independently on the resistojet concept considered, it is also necessary to analyze the two concepts separately, since they work at operational pressures on different orders of magnitude.

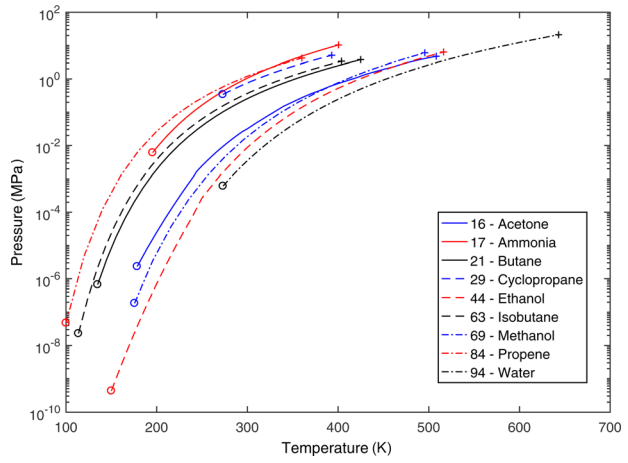

Fig. 3 Saturation curve. The circles means triple point and the crosses means critical point. The fluid is liquid on the left side of the curve, gaseous on its right side.

4.1 VLM Performance. To analyze the VLM performance some assumptions are needed. The VLM design characteristics have been taken according to the current design of TU Delft's VLM [9], where the nozzle expansion ratio (A_e/A^*) is 11, the chamber pressure (P_c) varies from 200 kPa to 500 kPa, and the chamber temperature varies within different ranges depending on the fluid, as shown by Tables 3 and 4. These chamber temperature ranges are the average maximum and minimum commonly found in literature for VLMs [7,8,25–27]. In addition, it is assumed that at the inlet of the micro-resistojet chamber, before heating, the propellant temperature is 283.16 K.

Figure 4 presents the needed enthalpy to increase the propellant temperature under the given conditions. Some fluids, in the initial conditions considered here (283.16 K and 200 kPa), are still liquid and need a phase change to become gaseous. This leads to a significantly higher required enthalpy to achieve their final temperature.

Under the above-explained assumptions, Fig. 5 shows the ranges of heating power and specific impulse for each propellant. Ammonia shows the best performance or, in other words, a higher specific impulse with a lower power consumption.

4.2 LPM Performance. To analyze the LPM performance some assumptions are also needed. The LPM characteristics have been taken according to the current design of TU Delft's LPM, with a grid of 67×67 circular microchannels with an aspect ratio of 5 in a 10×10 mm heater chip area [28]. The total cross-

Table 3 Chamber temperature, mass flow rate and thrust obtained with different propellants, for chamber pressures of 200 kPa (VLM case)

Propellant	T (K)	$\dot{m}$ (mg/s)	$\Im$ (mN)
16—Acetone	360–550	2.79–2.25	1.82
17—Ammonia	300–550	1.75–1.29	1.69
21—Butane	300–550	3.03–2.24	1.83
29—Cyclopropane	300–550	2.65–1.96	1.76
44—Ethanol	370–550	2.46–2.01	1.80
63—Isobutane	300–550	3.07–2.27	1.79
69—Methanol	360–550	2.13–1.73	1.74
84—Propene	300–550	2.62–1.94	1.79
94—Water	400–550	1.56–1.33	1.69

Table 4 Chamber temperature, mass flow rate, and thrust obtained with different propellants, for chamber pressures of 500 kPa (VLM case)

Propellant	T (K)	$\dot{m}$ (mg/s)	$\Im$ (mN)
16—Acetone	400–550	6.59–5.62	4.54
17—Ammonia	300–550	4.37–3.23	4.23
21—Butane	330–550	7.22–5.59	4.58
29—Cyclopropane	300–550	6.63–4.90	4.41
44—Ethanol	400–500	5.90–5.04	4.51
63—Isobutane	320–550	7.44–5.67	4.49
69—Methanol	390–550	5.13–4.32	4.35
84—Propene	300–550	6.56–4.84	4.47
94—Water	430–550	3.76–3.33	4.22

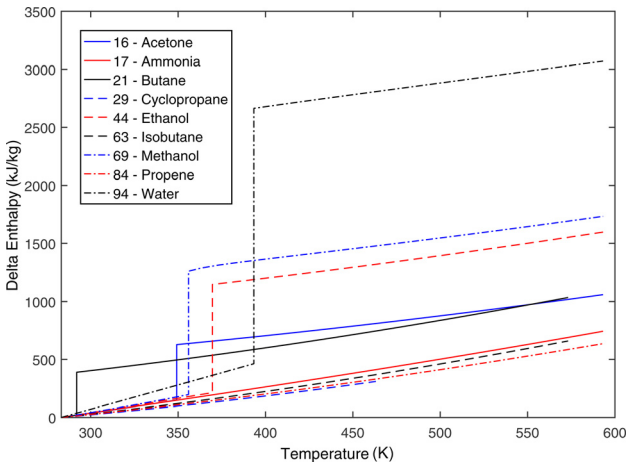

Fig. 4 Delta enthalpy for each propellant, at a chamber pressure of 200 kPa, as a function of the desired final chamber temperature

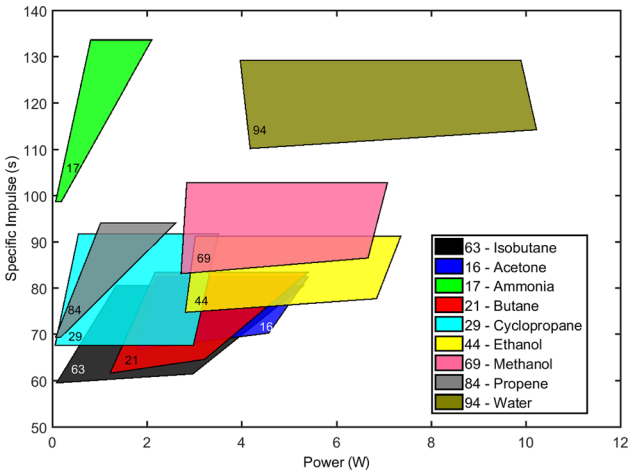

Fig. 5 Specific impulse versus heating power for various propellants (VLM case) according to the variations of temperature and pressure considered in Tables 3 and 4

sectional exit area (A_e) of the channels is equal to 10,000 μm^2, and the transmission coefficient for this kind of holes is equal to 0.19 [29]. The temperature varies from 300 to 700 K, and the plenum pressure from 50 Pa to 300 Pa. These values are the average maximum and minimum commonly found in the literature

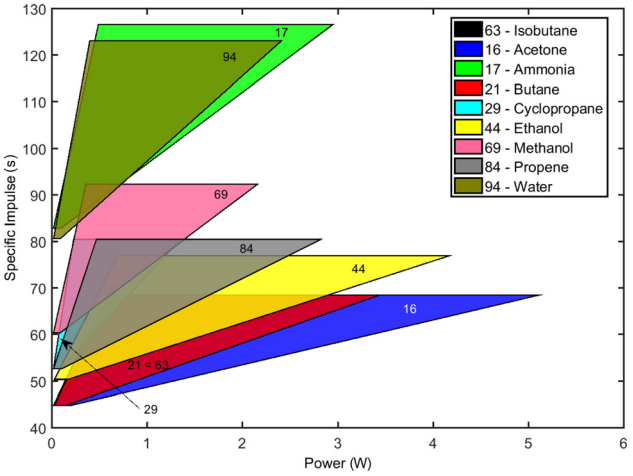

Fig. 6 Specific impulse versus heating power for various propellants (LPM case) according to the variations of temperature and pressure considered in Table 5

Table 5 Mass flow rate obtained with different propellants for a temperature range from 300 to 700 K and two different pressures (LPM case)

Propellant	$\dot{m}$ for 50 Pa (mg/s)	$\dot{m}$ for 300 Pa (mg/s)
16—Acetone	0.89	5.34
17—Ammonia	0.48	2.89
21—Butane	0.89	5.34
29—Cyclopropane	0.76	4.55
44—Ethanol	0.79	4.76
63—Isobutane	0.89	5.34
69—Methanol	0.66	3.97
84—Propene	0.76	4.55
94—Water	0.50	2.98

regarding LPMs [23,30–32]. In addition, it is assumed again that at the inlet of the plenum, the temperature is 283.16 K.

Under those assumptions, Fig. 6 shows the relation between heating power and specific impulse for each propellant. Ammonia and water show the best performance in this case, as they provide a high specific impulse with a similar level of required power as the others.

Table 5 presents the mass flow rate for the plenum pressure of 50 and 300 Pa, and for a range of wall temperatures from 300 to 700 K. It is important to emphasize that according to the theory presented in Sec. 3.2, the temperature does not affect the mass flow rate. Additionally, the thrust range varies from 0.39 to 3.59 mN independently of the kind of fluid, depending only on the setting of temperature and pressure.

5 Discussion

Performance, although very important in the design of propulsion systems, is not always the main criterion in the selection of a design option. Safety is also very important and has to be taken into account when designing micropropulsion systems, recalling that they are usually designed for small missions that have limitations in the budget or are for educational purposes. The former results in a need for reducing any costs related to the use of dedicated facilities or special equipment for handling the propellant, and the latter is to assure the safety of students and researchers.

5.1 Performance. In terms of performance, as anticipated in the previous sections, it is possible to rank the propellants

according to different parameters. In terms of thrust for the VLM, although the values are quite similar, it can be seen in Tables 3 and 4 that acetone and butane present the best values, and ammonia and water present the worst values. For the LPM, the values are the same independently on the kind of propellant. However, more important performance parameters for a propellant are the specific impulse and the power consumption. Figures 5 and 6 show that ammonia, water, and methanol present the highest specific impulse values in both propulsion systems. The power consumptions are quite similar when looking at the LPM, while in the VLM, we can see a higher power consumption for water and methanol than ammonia. This is easily explained by the fact that a phase change is not needed for ammonia, since it is already gaseous into the thruster. A complementary analysis is done in Sec. 5.4, where the Delta-V will also be taken into account.

5.2 Safety. Table 6 shows the selected propellants level in terms of flammability, health hazard, and instability. They do not present instability issues, with the exception of propene that can become unstable at elevated temperatures and pressures. As a conclusion, instability is not expected to be a major aspect to be taken into account in the selection process.

Most of the selected propellants present a low level of health hazard, meaning that exposure to them may cause irritation with only minor residual injury, and water and isobutane do not present any health hazard. On the other hand, Ammonia has the highest level of health hazard, with short exposure causing serious, temporary, or moderate residual injury. In summary, the choice of ammonia as a propellant should be done only if the facilities and operators are well equipped to safely handle it.

All the organic fluids considered have high or even extreme level of flammability, meaning that they can be easily ignited under ambient temperature conditions. Water does not present any flammability, and ammonia presents a low level of flammability, since it requires considerable preheating before ignition. As it is well known, having fire means meeting the fire triangle (oxygen, fuel, and heat), so this criterion should be analyzed from different perspectives when applied to micro-resistojets. When the satellite is in orbit, it is very unlikely to have ignition since there is no oxygen; thus, there are no threats for the system. Even though during launch the tank is well sealed with very low possibility to leak, it could be an issue due to the restriction posed by the main payload. However, flammability may become an important issue while handling the propellant. The fluids with an extreme level of flammability have to be very carefully handled by well-trained operators, into well-equipped facilities since those substances will rapidly vaporize at normal atmospheric pressure and temperature, or are rapidly dispersed in air where they could burn readily.

5.3 System Density. Table 7 presents the density of the considered propellants in their liquid state, at a pressure of 1 MPa and temperature lower than 293.15, the assumed best-case conditions into the tank. The lowest density is obtained for propene and the highest is for Water. Roughly speaking, Water fills the same volume with double the mass than Propene. Basically, from the miniaturization point of view, highest density is obviously the best case, because it allows for a higher propellant mass in the same volume.

Table 6 Safety characteristics of the selected propellants

Propellant	Flammability	Health hazard	Instability
16—Acetone	High	Low	N/A
17—Ammonia	Low	High	N/A
21—Butane	Extreme	Low	N/A
29—Cyclopropane	Extreme	Low	N/A
44—Ethanol	High	Low	N/A
63—Isobutane	Extreme	N/A	N/A
69—Methanol	High	Low	N/A
84—Propene	Extreme	Low	Low
94—Water	N/A	N/A	N/A

Table 7 Density of the considered fluids, in their liquid state at a pressure of 1 MPa

Propellant	Density (kg/m^3)
16—Acetone	791
17—Ammonia	610.33
21—Butane	579.88
29—Cyclopropane	627.53
44—Ethanol	789
63—Isobutane	558.24
69—Methanol	791.88
84—Propene	514.31
94—Water	998.62

5.4 Final Considerations. The last comparison that needs to be done is related to velocity increments (ΔV) achieved with different fluids. This is an important parameter to estimate the performance of the propulsion system, when installed in a specific spacecraft. For cases when the propellant mass used is significantly small compared to the total spacecraft mass ($(M_p/M) \ll 1$), the Delta-V can be calculated by using the linear approximation of the rocket equation

$$\Delta V = g_0 I_{sp} \frac{M_p}{M} \tag{10}$$

where M is the initial spacecraft mass and M_p is the propellant mass.

Considering a nanosatellite of 3.6 kg that will perform a formation flying mission with the requirements indicated in Sec. 2, Figs. 7 and 8 present the Delta-V per volume of propellant needed, as a function of the heating power, for the two resistojet concepts considered. In both cases, water provides the best Delta-V per volume. For the VLM, water has also the highest power consumption, but this does not apply to the LPM, which presents similar power consumption for almost all propellants as we can see in Fig. 8. This difference is due to the relatively high energy of vaporization of water which is needed in the process of the

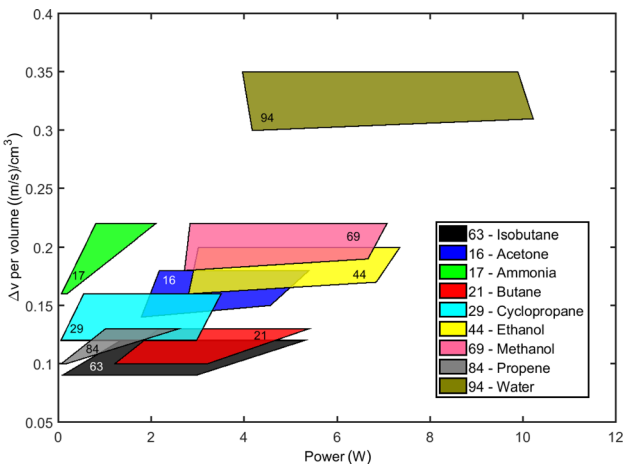

Fig. 7 ΔV per volume of fluid versus heating power (VLM case)

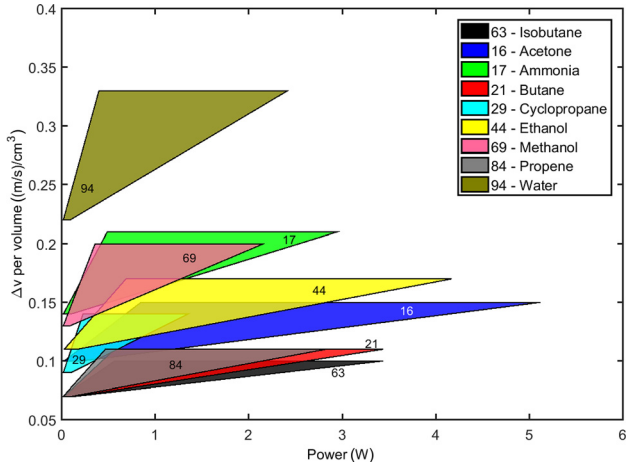

Fig. 8 ΔV per volume of fluid versus heating power (LPM case)

VLM, while in the LPM, due to the low pressure in the plenum, the water is already in a gaseous state in that part of the propulsion system.

All the selected propellants have a potential to be selected for the specific mission requirements considered in this paper. However, water shows to be the most promising one, especially for the LPM. It scores very high in all the criteria considered, even though the power consumption is higher in the VLM case. It presents the highest ΔV per unit volume and no safety issues. Ammonia is, in fact, the superior one in terms of ΔV and power for the VLM. However, it presents the highest level of hazard that might be not appropriate for a large number of small satellite missions.

6 Conclusions

A selection methodology was proposed to compare fluids that could be promising choices as propellant for micro-resistojets. This methodology helped in narrowing down the number of choices from 95 fluids in the beginning to nine that were analyzed in depth and discussed in terms of performance and safety. It can also be extended to other applications with different micropropulsion systems or other types of propellant.

It is shown that water is the most promising propellant for both micro-resistojet concepts considered. Even though it has a higher power consumption, it also has the best velocity increment per volume of propellant, almost twice higher than all the other analyzed fluids. Another important aspect is that water is the safest propellant, and the easiest one to handle and acquire. However, other propellants from the top nine lists might be interesting for other applications or missions.

Finally, this paper and the analysis presented here can be considered as a reference for future developments of micropropulsion systems and, in particular, micro-resistojets.

Acknowledgment

The authors would like to express their sincere gratitude to the TU Delft Space Institute and the academic staff of the Space Systems Engineering chair of the Faculty of Aerospace Engineering at TU Delft.

The research reported in this publication was supported by CNPq (Conselho Nacional de Desenvolvimento Científico e Tecnológico, Brasil) and CEFET-RJ (Centro Federal de Educação Tecnológica Celso Suckow da Fonseca do Rio de Janeiro).

Nomenclature

A_e = thruster exit area (m^2)
A^* = nozzle throat area (m^2)
$\bar{c} = \sqrt{8kT/\pi m}$ = mean thermal speed (m/s)
FL = first level of the selection criteria
g_0 = Earth gravitational acceleration at sea level (m/s^2)
i = the selection criteria
I_{sp} = specific impulse (s)
k = Boltzmann constant (J/kg)
Kn = Knudsen number (dimensionless)
L_0 = characteristic dimension (m)
m = mass (kg)
$\dot{m}$ = mass flow rate (kg/s)
M_w = molecular mass (kg/mol)
P_a = ambient pressure (Pa)
P_c = chamber pressure (Pa)
P_e = pressure at the nozzle exit (Pa)
P_0 = plenum pressure (Pa)
R_A = universal gas constant 8.3144598 (J/(mol K))
SL = second level of the selection criteria
T = temperature (K)
T_c = chamber temperature (K)
T_w = channel wall temperature (K)
T_0 = plenum temperature (K)
u_e = exit velocity (m/s)
WF = weight factor of the selection criteria
WF_{max} = maximum weight factor of the selection criteria
α = transmission coefficient (dimensionless)
γ = specific heat ratio (dimensionless)
Γ = Vandenkerckhove function (dimensionless)
λ = mean free path (m)
$\Im$ = thrust (N)

Appendix: Propellant Candidates

Table 8 This table presents all propellant candidates that were analyzed in this paper

No.	Fluid name	Chemical formula	M_w (g/mol)	Ref.	Selection step
1	1,1,1,2,3,3,3-Heptafluoropropane (R227ea)	C_3HF_7	170.03	[33]	3—AHP and Pugh matrix
2	1,1,1,2,3,3-Hexafluoropropane (R236ea)	$C_3H_2F_6$	152.04	[33]	3—AHP and Pugh matrix
3	1,1,1,3,3,3-Hexafluoropropane (R236fa)	$C_3H_2F_6$	152.04	[33]	3—AHP and Pugh matrix
4	1,1,1,3,3-Pentafluoropropane (R245fa)	$C_3H_3F_5$	134.05	[33]	3—AHP and Pugh matrix
5	1,1,2,2,3-Pentafluoropropane (R245ca)	$C_3H_3F_5$	134.05	[33]	3—AHP and Pugh matrix
6	1,1,2-Trichloro-1,2,2-trifluoroethane (R113)	$C_2Cl_3F_3$	187.38	[33,34]	3—AHP and Pugh matrix
7	1,1-Dichloro-1-fluoroethane (R141b)	$C_2H_3Cl_2F$	116.94	[33]	3—AHP and Pugh matrix
8	1,2-Dichloro-1,1,2,2-tetrafluoroethane (R114)	$C_2Cl_2F_4$	170.92	[33,34]	3—AHP and Pugh matrix
9	1-Chloro-1,1-difluoroethane (R142b)	$C_2H_3ClF_2$	100.49	[33]	3—AHP and Pugh matrix
10	2,2-Dimethylpropane	C_5H_{12}	72.15	[33]	3—AHP and Pugh matrix
11	2,4-xylidine	$C_8H_{11}N$	121.18	[33,34]	3—AHP and Pugh matrix
12	2-Methylbutane	C_5H_{12}	72.15	[33]	3—AHP and Pugh matrix
13	2-Methylpentane	C_6H_{14}	86.18	[33]	3—AHP and Pugh matrix
14	3-3'-diaminopropylamine	$C_5H_{14}N_2$	102.18	[33,34]	3—AHP and Pugh matrix

Table 8 (continued)

No.	Fluid name	Chemical formula	M_w (g/mol)	Ref.	Selection step
15	Acetic acid	$C_2H_4O_2$	60.05	[35]	3—AHP and Pugh matrix
16	Acetone	C_3H_6O	58.08	[35]	4—Analysis
17	Ammonia	NH_3	17.03	[33,34]	4—Analysis
18	Aniline	$C_6H_5NH_2$	93.13	[33,34]	3—AHP and Pugh matrix
19	Argon	Ar	39.95	[33,34]	2—Feasibility assessment
20	Benzene	C_6H_6	78.11	[33]	3—AHP and Pugh matrix
21	Butane	C_4H_{10}	58.12	[33]	4—Analysis
22	Carbon dioxide	CO_2	44.01	[33,34]	2—Feasibility assessment
23	Carbon monoxide	CO	21.01	[33,34]	2—Feasibility assessment
24	Carbonyl sulfide	COS	60.07	[33]	2—Feasibility assessment
25	Chlorine	Cl_2	70.1	[33,34]	2—Feasibility assessment
26	Chloropentafluoroethane (R115)	C_2ClF_5	154.47	[33,34]	3—AHP and Pugh matrix
27	Chlorotrifluoromethane (R13)	$CClF_3$	104.46	[33,34]	2—Feasibility assessment
28	Cyclohexane	C_6H_{12}	84.16	[33]	3—AHP and Pugh matrix
29	Cyclopropane	C_3H_6	42.08	[33,34]	4—Analysis
30	Decafluorobutane	C_4F_{10}	238.03	[33]	3—AHP and Pugh matrix
31	Decane	$C_{10}H_{22}$	142.29	[33]	3—AHP and Pugh matrix
32	Dichlorodifluoromethane (R12)	CCl_2F_2	120.91	[33,34]	3—AHP and Pugh matrix
33	Dichlorofluoromethane (R21)	$CHCl_2F$	102.92	[33,34]	3—AHP and Pugh matrix
34	Dinitrogen monoxide	N_2O	44.01	[33]	2—Feasibility assessment
35	Dodecafluoropentane	C_5F_{12}	288.04	[33]	3—AHP and Pugh matrix
36	Dodecane	$C_{12}H_{26}$	170.34	[33]	3—AHP and Pugh matrix
37	Ethane	C_2H_6	30.07	[33,34]	2—Feasibility assessment
38	Ethane, 1,1,1,2-tetrafluoro- (R134a)	CH_2FCF_3	102.03	[33,34]	3—AHP and Pugh matrix
39	Ethane, 1,1,1-trifluoro- (R143a)	$C_2H_3F_3$	84.04	[33,34]	2—Feasibility assessment
40	Ethane, 1,1-difluoro- (R152a)	$C_2H_4F_2$	66.05	[33,34]	3—AHP and Pugh matrix
41	Ethane, 1-chloro-1,2,2,2-tetrafluoro- (R124)	C_2HClF_4	136.48	[33]	3—AHP and Pugh matrix
42	Ethane, 2,2-dichloro-1,1,1-trifluoro- (R123)	$C_2HCl_2F_3$	152.93	[33]	3—AHP and Pugh matrix
43	Ethane, pentafluoro- (R125)	C_2HF_5	120.02	[33]	2—Feasibility assessment
44	Ethanol	C_2H_6O	46.07	[35]	4—Analysis
45	Ethene	C_2H_4	28.05	[33]	2—Feasibility assessment
46	Ethyl formate	$C_3H_6O_2$	74.08	[35]	3—AHP and Pugh matrix
47	Ethyl nitrate	$C_2H_5NO_3$	91.07	[33,36]	3—AHP and Pugh matrix
48	Ethylammonium nitrate	$C_2NH_8NO_3$	108.1	[33,36]	3—AHP and Pugh matrix
49	Ethylenoxide	C_2H_4O	44.05	[33,36]	3—AHP and Pugh matrix
50	Fluorine	Fe_2	72	[33,34]	2—Feasibility assessment
51	Fluoromethane (R41)	CH_3F	34.03	[33,34]	2—Feasibility assessment
52	Furfuryl alcohol	$C_5H_6O_2$	98.1	[33,36]	3—AHP and Pugh matrix
53	Helium	He	4	[33]	2—Feasibility assessment
54	Heptane	C_7H_{16}	100.21	[33]	3—AHP and Pugh matrix
55	Hexafluoroethane (R116)	C_2F_6	138.01	[33]	2—Feasibility assessment
56	Hexane	C_6H_{14}	86.18	[33]	3—AHP and Pugh matrix
57	Hydrazine	N_2H_4	32.05	[35]	3—AHP and Pugh matrix
58	Hydrogen	H_2	2.02	[33,34]	2—Feasibility assessment
59	Hydrogen chloride	HCl	36.46	[33,34]	2—Feasibility assessment
60	Hydrogen cyanide	HCN	27.03	[35]	3—AHP and Pugh matrix
61	hydrogen peroxide	H_2O_2	34.01	[33]	3—AHP and Pugh matrix
62	Hydrogen sulfide	H_2S	34.08	[33,34]	2—Feasibility assessment
63	Isobutane	C_4H_{10}	58.12	[33,34]	4—Analysis
64	Krypton	Kr	83.8	[33]	2—Feasibility assessment
65	Limonene	$C_{10}H_{16}$	136.24	[37]	3—AHP and Pugh matrix
66	Methane	CH_4	16.04	[33,34]	2—Feasibility assessment
67	Methane, chlorodifluoro- (R22)	$CHClF_2$	86.47	[33,34]	3—AHP and Pugh matrix
68	Methane, difluoro- (R32)	CH_2F_2	52.02	[33,34]	2—Feasibility assessment
69	Methanol	CH_4O	32.04	[33]	4—Analysis
70	Monomethylamine	CH_5N	31.06	[33,36]	2—Feasibility assessment
71	Neon	Ne	20.18	[33]	2—Feasibility assessment
72	Nitric acid	HNO_3	63.01	[35]	3—AHP and Pugh matrix
73	Nitric oxide	NO	30.01	[33,34]	2—Feasibility assessment
74	Nitrogen	N_2	28.01	[33,34]	2—Feasibility assessment
75	Nitrogen trifluoride	NF_3	71	[33]	2—Feasibility assessment
76	Nonane	C_9H_{20}	128.2	[33]	3—AHP and Pugh matrix
77	Nitrous oxide	NO_2	44.01	[38]	2—Feasibility assessment
78	Octafluorocyclobutane (RC318)	C_4F_8	200.03	[33]	3—AHP and Pugh matrix
79	Octafluoropropane (R218)	C_3F_8	188.02	[33]	3—AHP and Pugh matrix
80	Octane	C_8H_{18}	114.23	[33]	3—AHP and Pugh matrix
81	Oxygen	O_2	32	[33,34]	2—Feasibility assessment
82	Pentane	C_5H_{12}	72.15	[33]	3—AHP and Pugh matrix
83	Propane	C_3H_8	44.1	[33,34]	3—AHP and Pugh matrix
84	Propene	C_3H_6	42.08	[33,34]	4—Analysis
85	Propyne	C_3H_4	40.06	[33,34]	3—AHP and Pugh matrix
86	Sulfur dioxide	SO_2	64.07	[33,34]	3—AHP and Pugh matrix
87	Sulfur hexafluoride	SF_6	146.06	[33,34]	2—Feasibility assessment

Table 8 (continued)

No.	Fluid name	Chemical formula	M_w (g/mol)	Ref.	Selection step
88	Tetrafluoromethane (R14)	CF_4	88	[33]	2—Feasibility assessment
89	Tetranitromethane	CN_4O_8	196.04	[33,36]	3—AHP and Pugh matrix
90	Toluene	C_7H_8	92.14	[33]	3—AHP and Pugh matrix
91	Trichlorofluoromethane (R11)	CCl_3F	137.37	[33]	3—AHP and Pugh matrix
92	Trifluoromethane (R23)	CHF_3	70.01	[33]	2—Feasibility assessment
93	Trimethylaluminium	$C_6H_{18}Al_2$	144.17	[33,36]	3—AHP and Pugh matrix
94	Water	H_2O	18.02	[33]	4—Analysis
95	Xenon	Xe	131.29	[33,34]	2—Feasibility assessment

References

[1] Selva, D., and Krejci, D., 2012, "A Survey and Assessment of the Capabilities of Cubesats for Earth Observation," Acta Astronaut., **74**, pp. 50–68.

[2] Boshuizen, C. R., Mason, J., Klupar, P., and Spanhake, S., 2014, "Results From the Planet Labs Flock Constellation," AIAA Paper No. SSC14-I-1.

[3] Guo, J., Bouwmeester, J., and Gill, E., 2016, "In-Orbit Results of Delfi-n3Xt: Lessons Learned and Move Forward," Acta Astronaut., **121**, pp. 39–50.

[4] Ciaralli, S., Coletti, M., and Gabriel, S. B., 2016, "Results of the Qualification Test Campaign of a Pulsed Plasma Thruster for Cubesat Propulsion (PPTCUP)," Acta Astronaut., **121**, pp. 314–322.

[5] Coletti, M., Guarducci, F., and Gabriel, S., 2011, "A Micro PPT for Cubesat Application: Design and Preliminary Experimental Results," Acta Astronaut., **69**(3–4), pp. 200–208.

[6] Köhler, J., Bejhed, J., Kratz, H., Bruhn, F., Lindberg, U., Hjort, K., and Stenmark, L., 2002, "A Hybrid Cold Gas Microthruster System for Spacecraft," Sens. Actuators A, **97–98**, pp. 587–598.

[7] Cheah, K. H., and Low, K.-S., 2015, "Fabrication and Performance Evaluation of a High Temperature Co-Fired Ceramic Vaporizing Liquid Microthruster," J. Micromech. Microeng., **25**(1), p. 015013.

[8] Kundu, P., Bhattacharyya, T. K., and Das, S., 2012, "Design, Fabrication and Performance Evaluation of a Vaporizing Liquid Microthruster," J. Micromech. Microeng., **22**(2), p. 025016.

[9] Cervone, A., Zandbergen, B., Guerrieri, D. C., De Athayde Costa e Silva, M., Krusharev, I., and van Zeijl, H., 2017, "Green Micro-Resistojet Research at Delft University of Technology: New Options for Cubesat Propulsion," CEAS Space J., **9**(1), pp. 111–125.

[10] Ketsdever, A. D., and Micci, M. M., 2000, *Micropropulsion for Small Spacecraft*, Vol. 187, AIAA, Reston, VA.

[11] Mike Meyer, L. J., 2015, "NASA Technology Roadmaps, TA 2: In-Space Propulsion Technologies," NASA, Washington, DC.

[12] ESA, 2015, "European Space Technology Master Plan," ESA, Noordwijk, The Netherlands.

[13] Gohardani, A. S., Stanojev, J., Demairé, A., Anflo, K., Persson, M., Wingborg, N., and Nilsson, C., 2014, "Green Space Propulsion: Opportunities and Prospects," Prog. Aerosp. Sci., **71**, pp. 128–149.

[14] Anflo, K., and Möllerberg, R., 2009, "Flight Demonstration of New Thruster and Green Propellant Technology on the PRISMA Satellite," Acta Astronaut., **65**(9–10), pp. 1238–1249.

[15] Amri, R., and Gibbon, D., 2012, "In Orbit Performance of Butane Propulsion System," Adv. Space Res., **49**(4), pp. 648–654.

[16] Rankin, D., Kekez, D. D., Zee, R. E., Pranajaya, F. M., Foisy, D. G., and Beattie, A. M., 2005, "The CanX-2 Nanosatellite: Expanding the Science Abilities of Nanosatellites," Acta Astronaut., **57**(2–8), pp. 167–174.

[17] Zakirov, V., Sweeting, M., Lawrence, T., and Sellers, J., 2001, "Nitrous Oxide as a Rocket Propellant," Acta Astronaut., **48**(5), pp. 353–362.

[18] Sutton, G. P., and Biblarz, O., 2010, *Rocket Propulsion Elements*, 8th ed., Wiley, Hoboken, NJ.

[19] Zahedi, F., 1986, "The Analytic Hierarchy Process: A Survey of the Method and Its Applications," Interfaces, **16**(4), pp. 96–108.

[20] Pugh, S., 1991, *Total Design: Integrated Methods for Successful Product Engineering*, Addison-Wesley, Harlow, England.

[21] Cervone, A., Deeb, A., van Wees, T., Jansen, E., Sundaramoorthy, P., Chu, J., and Zandbergen, B., 2015, "A Micro-Propulsion Subsystem to Enable Formation Flying on the DelFFi Mission," Eighth International Workshop on Satellite Constellations and Formation Flying (IWSCFF), IAF, Delft, The Netherlands, June 8–10, pp. 1–15.

[22] NFPA, 2010, "Fire Protection Guide to Hazardous Materials," National Fire Protection Association, Quincy, MA.

[23] Ketsdever, A. D., Lee, R. H., and Lilly, T. C., 2005, "Performance Testing of a Microfabricated Propulsion System for Nanosatellite Applications," J. Micromech. Microeng., **15**(12), p. 2254.

[24] Guerrieri, D. C., Cervone, A., and Gill, E., 2016, "Analysis of Nonisothermal Rarefied Gas Flow in Diverging Microchannels for Low-Pressure Microresistojets," ASME J. Heat Transfer, **138**(11), p. 112403.

[25] Cen, J., and Xu, J., 2010, "Performance Evaluation and Flow Visualization of a MEMS Based Vaporizing Liquid Micro-Thruster," Acta Astronaut., **67**(3–4), pp. 468–482.

[26] Chen, C.-C., Liu, C.-W., Kan, H.-C., Hu, L.-H., Chang, G.-S., Cheng, M.-C., and Dai, B.-T., 2010, "Simulation and Experiment Research on Vaporizing Liquid Micro-Thruster," Sens. Actuators A, **157**(1), pp. 140–149.

[27] Karthikeyan, K., Chou, S. K., Khoong, L. E., Tan, Y. M., Lu, C. W., and Yang, W. M., 2012, "Low Temperature Co-Fired Ceramic Vaporizing Liquid Microthruster for Microspacecraft Applications," Appl. Energy, **97**, pp. 577–583.

[28] Guerrieri, D. C., de Athayde Costa e Silva, M., Zandbergen, B. T. C., and Cervone, A., 2015, "Development of a Low Pressure Free Molecular Micro-Resistojet for CubeSat Applications," 66th International Astronautical Congress (IAC), International Astronautical Federation, Jerusalem, Israel.

[29] Lafferty, J. M., 1998, *Foundations of Vaccum Science and Technology*, Wiley, Hoboken, NJ.

[30] Ahmed, Z., Gimelshein, S. F., and Ketsdever, A., 2005, "Numerical Analysis of Free Molecule Micro-Resistojet Performance," AIAA Paper No. 2005-4262.

[31] Lee, R., Bauer, A., Killingsworth, M., Lilly, T., Duncan, J., and Ketsdever, A., 2007, "Performance Characterization of the Free Molecule Micro-Resistojet Utilizing Water Propellant," AIAA Paper No. 2007-5185.

[32] Palmer, K., Nguyen, H., and Thornell, G., 2013, "Fabrication and Evaluation of a Free Molecule Micro-Resistojet With Thick Silicon Dioxide Insulation and Suspension," J. Micromech. Microeng., **23**(6), p. 065006.

[33] Linstrom, P., and Mallard, W., 2016, "NIST Chemistry Webbook," NIST Standard Reference Database No. 69, NIST, Gaithersburg, MD, accessed Apr. 15, 2016, http://webbook.nist.gov

[34] Air Liquide, "Gas Encyclopedia," Air Liquide, Paris, France, accessed Apr. 15, 2016, http://encyclopedia.airliquide.com/

[35] Perry, R. H., and Green, D. W., 2008, *Perry's Chemical Engineers' Handbook*, 8th ed., McGraw-Hill, New York.

[36] Green Advanced Space Propulsion, 2011, "Green Propellant Candidates of GRASP," European Commission, Brussels, Belgium, accessed May 9, 2017, http://cordis.europa.eu/project/rcn/89683_en.html#top

[37] Díaz, M. E., Guetachew, T., Landy, P., Jose, J., and Voilley, A., 1999, "Experimental and Estimated Saturated Vapour Pressures of Aroma Compounds," Fluid Phase Equilib., **157**(2), pp. 257–270.

[38] Ferreira, A., and Lobo, L., 2009, "Nitrous Oxide: Saturation Properties and the Phase Diagram," J. Chem. Thermodyn., **41**(12), pp. 1394–1399.